Electronic Supplementary Material (ESI) for Environmental Science: Nano.

Supplemental Material for: "Do Potential Dependent Kinetics Play a Role In Photocatalytic Rate Trends?"

Kirk H. Bevan
Division of Materials Engineering, Faculty of Engineering, McGill University, Montréal, Québec, Canada and Centre for the Physics of Materials, McGill University, Montréal, Québec, Canada

Laurence M. Peter
Department of Chemistry, University of Bath, Bath BA2 7AY, United Kingdom

Premable

All citations/references below are the same as those (in ordering and listing) provided within the main manuscript.

A. Hematite Results

The same physical model presented in the main manuscript can be applied to other photoanodes by simply adjusting the model parameters to values suitable for a given material system. In Fig. S1 we show the numerical results for a Fe_2O_3-water photoanode, where it can be seen that the emergence of a p_s-to-p_s^3 transition is again obtained through the inclusion of a Tafel parameter. The sloping saturation regime in Fig. S1a results from the fact that the depletion region width in hematite (at a doping of $N_D = 1 \times 10^{19}/\text{cm}^3$) is not sufficient to capture all photo-generated holes [5]. This also explains why the photo-generated current does not reach the maximum defined by the incident photon flux – reaching only $\sim 1/4$ of 3 Suns at maximum illumination in Fig. S1a. Moreover, the p_s-to-p_s^3 trend is robust against changes in the applied bias and the electrode doping density as can be seen in Fig. S1c. There is, however, a shift in the trend with respect to doping density in Fig. S1c. This also arises from the shortened depletion region at higher doping densities as can be seen in Fig. S1d where we use the photon flux (Φ) on the vertical axis. For the same photon flux, reading over from the vertical axis, less holes are swept to the depletion region interface (measured by p_s) when the doping is higher and the semiconductor depletion region width is correspondingly smaller. Thus, there is a shift in the p_s-to-p_s^3 with respect to doping for a planar electrode. In a nano-structured electrode photon absorption is more complex and this trend is likely to be less pronounced as nano-structuring provides more opportunities for light absorption and internal scattering. In a planar electrode, at sufficiently low doping the light penetration depth is fully encompassed by the depletion region and there is no further shift to the right in the profiles provided by Fig. S1d. Lastly, the p_s-to-p_s^3 trend is also reproduced by the analytical model when applied to Fe_2O_3 as shown in Fig. S2.

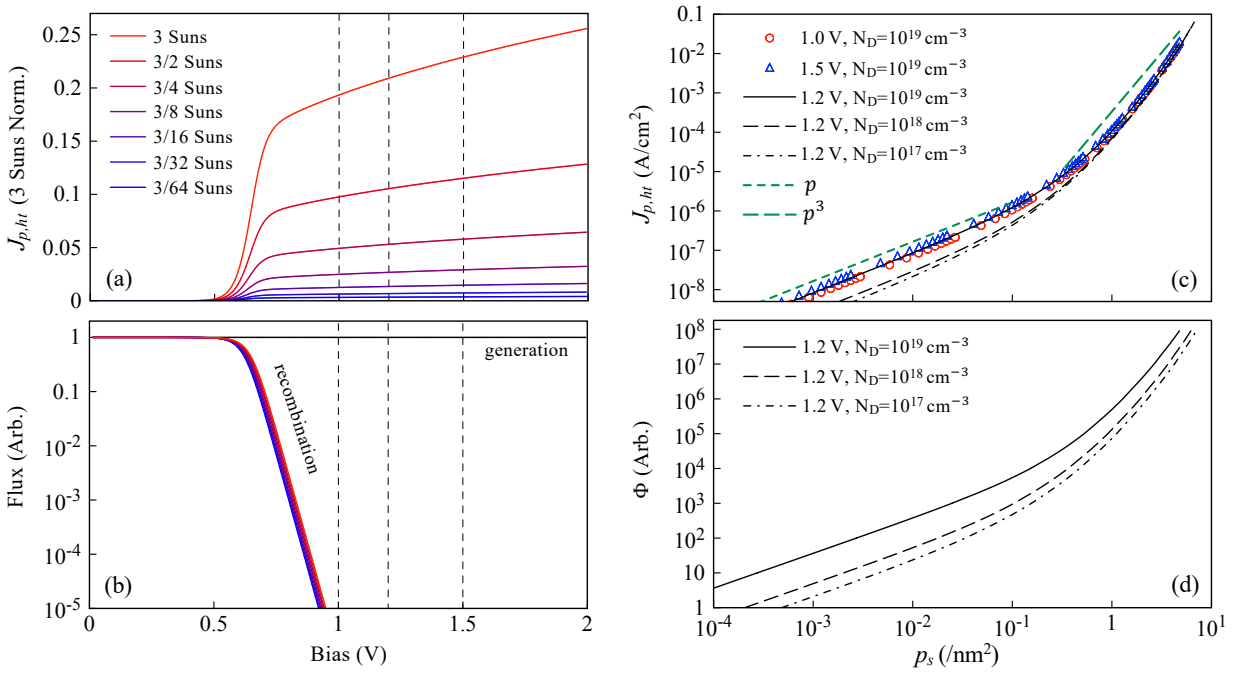

FIG. S1. Results calculated for a planar Fe_2O_3 thin film electrode assuming a Tafel coefficient of $\gamma = 0.6$. (a) Variation in the illumination current with respect to light intensity (normalized by dividing by 3 Suns of intensity) for $N_D = 1 \times 10^{19}/\text{cm}^3$, the biases at which surface hole density plots are obtained are indicated as vertical dashed lines. (b) All plots of the surface hole concentration with respect to a reaction quantity are taken beyond onset where band bending sufficiently suppresses recombination (blue through red) with respect to the captured light flux (black). (c) The hole transfer current with respect to the surface hole density (p_s) at various biases and doping concentrations, p_s-to-p_s^3 fits are provided as guides to the eye. (d) Trends with respect to the incident flux, normalized by the minimum flux applied (which is the same for all curves), and surface hole concentration p_s. The maximum flux (Φ) applied, in all results, corresponds to 3 Suns.

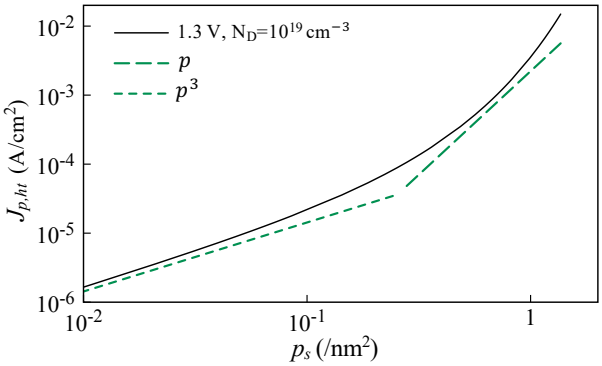

FIG. S2. Analytical results for a planar Fe_2O_3 thin film electrode assuming a Tafel coefficient of $\gamma = 0.5$ for varying illumination intensities at a fixed bias of 1.3 V versus flat-band. In this plot the assumed analytical parameters are: $C_H = 100$ μF/cm^2, $k_{p0} = 10$ s^{-1}, $L_p = 10^{-7}$ cm, $\alpha = 1{\times}10^5$ cm^{-1}, $\beta = 0.5$, $k_{rec,0} = 10^7$ s^{-1}, $\epsilon_r = 25$ [4, 5].

B. Theoretical Model Parameter Values

All parameters pertaining to the analytical model can be found in the caption to each such figure. Below we provide the key material parameters utilized for the numerical simulations conducted. For Fe_2O_3 approximate values are employed where indicated, as there is no major impact on the general trends through the variation of such parameters (e.g., varying τ will merely shift the onset voltage). All other numerical parameters are set the same as discussed in Ref. 20.

TABLE S1. Numerical Model Parameters

Parameter (Units)	Fe_2O_3 System	$BiVO_4$ System	Description
E_G	2.1 eV [4, 5, 43]	2.4 eV [30]	semiconductor band gap
$\epsilon_{r,sc}$	25 [4, 5, 43]	7 [29]	semiconductor dielectric constant
$\epsilon_{r,L}$	80	80	water dielectric constant
c_{sup}	1 Mol	1 Mol	supporting electrolyte concentration
N_C	$\sim 4 \times 10^{19}$ cm^{-3} [24]	2.14×10^{19} cm^{-3}	conduction band effective density of states
N_V	$\sim 4 \times 10^{19}$ cm^{-3} [24]	1.47×10^{19} cm^{-3}	valence band effective density of states
α	$\sim 10^5$ cm^{-1} [4, 5, 43]	6×10^5 cm^{-1} [29]	photon absorption coefficient
τ	~ 40 ps	40 ps [30]	semiconductor carrier lifetime
k_{p0}	0.1 s^{-1} [10]	0.1 s^{-1} [10]	equilibrium hole transfer rate
γ	0.6	0.6	Tafel parameter

C. Further Comments on the Surface Hole Concentrations & Photocatalytic Rates

The nature of the "holes" detected spectroscopically in the case of hematite has been clarified by analysis of the infrared spectra using isotopic oxygen substitution [37]. It is clear than the holes are in fact located on the surface at Fe sites. The simplest chemical representation of the surface trapped hole is that it corresponds to >Fe=O, i.e., it is an Fe(IV) species. More recent DFT calculations suggest that the hole may be partly localized on the oxygen atom of the Fe-O moiety [13]. If, as seems probable, there is a pseudo-equilibrium between free and surface trapped holes in this case, the majority of holes will indeed be surface trapped since there is good evidence that the Fe=O state is located well above the valence band [38]. In the case where no surface trapping occurs (e.g. on defect-free silicon surfaces), computations show that holes are located in a very narrow surface region, so that the surface concentration model can be employed unless the doping is very high [39].

Moreover, the photo-oxidation of water is of course a 4-electron (or 4-hole) process that must involve surface-bound species. The identity of these species will depend on the nature of the photoanode. The treatment given in our paper does not consider the mechanistic complexity of the reaction, using instead a phenomenological rate constant for the overall reaction. A detailed analysis that takes into account specific mechanisms is beyond the scope of the paper, but we note in the paper that such an analysis in the case of hematite gives the same conclusion, namely that acceleration of hole transfer by changes in the potential drop in the Helmholtz layer needs to be considered when interpreting "reaction order" plots. A study on this is currently under preparation by L. Peter at the time of publication.

D. Numerical Model

The numerical model utilized in this work builds upon Ref. 20 and can be found via the link below:
`http://www.physics.mcgill.ca/~bevankh/Codes/SLJCompact/SLJCompact1.1.zip`

Within from the root directory of this zip-file, the analytical codes/examples can be found in:

- examples/BiVO4/Fig6/
- examples/Fe2O3/SupplementalFig2/

and only require Matlab to run.

[1] R. Quesada-Cabrera and I. P. Parkin, Frontiers in Chemistry, 2020, **8**, 817.
[2] S. K. Loeb, P. J. J. Alvarez, J. A. Brame, E. L. Cates, W. Choi, J. Crittenden, D. D. Dionysiou, Q. Li, G. Li-Puma, X. Quan, D. L. Sedlak, T. David Waite, P. Westerhoff and J.-H. Kim, Environ. Sci. Technol., 2019, **53**, 2937–2947.
[3] X. Yang and D. Wang, ACS Appl. Energy Mater., 2018, **1**, 6657–6693.
[4] L. Peter and K. Wijayantha, ChemPhysChem, 2014, **15**, 1983–1995.
[5] L. Peter, J. Solid State Electrochem., 2013, **17**, 315–326.
[6] M. Isaacs, J. Garcia-Navarro, W.-J. Ong and P. Jiménez-Calvo, Global Challenges, 2023, **7**, 2200165.
[7] A. Saravanan, P. S. Kumar, D.-V. N. Vo, P. R. Yaashikaa, S. Karishma, S. Jeevanantham, B. Gayathri and V. D. Bharathi, Environmental Chemistry Letters, 2021, **19**, 441–463.
[8] J. M. Coronado, in A Historical Introduction to Photocatalysis, ed. J. M. Coronado, F. Fresno, M. D. Hernández-Alonso and R. Portela, Springer London, London, 2013, pp. 1–4.
[9] R. Memming, Semiconductor Electrochemistry, WILEY-VCH Verlag GmbH&Co. KGaA, 2nd edn., 2015.
[10] C. A. Mesa, L. Francàs, K. R. Yang, P. Garrido-Barros, E. Pastor, Y. Ma, A. Kafizas, T. E. Rosser, M. T. Mayer, E. Reisner, M. Grätzel, V. S. Batista and J. R. Durrant, Nat. Chem., 2020, **12**, 82–89.
[11] C. A. Mesa, L. Rao, Reshma R. Francas, S. Corby and J. R. Durrant, Nat. Chem., 2020, **12**, 1099.
[12] C. A. Mesa et al., J. Am. Chem. Soc., 2017, **139**, 11537.
[13] G. Righi, J. Plescher, F.-P. Schmidt, R. K. Campen, S. Fabris, A. Knop-Gericke, R. Schlögl, T. E. Jones, D. Teschner and S. Piccinin, Nature Catalysis, 2022, **5**, 888.
[14] S. Zhang, W. Leng and K. Liu, Phys. Chem. Chem. Phys., 2023.
[15] S. Zhang and W. Leng, Nat. Chem., 2020, **12**, 1097–1098.
[16] L. M. Peter, A. B. Walker, T. Bein, A. G. Hufnagel and I. Kondofersky, Journal of Electroanalytical Chemistry, 2020, **872**, 114234.
[17] Electrochemical Methods: Fundamentals and Applications, Bard, Allen J. and Faulkner, Larry R., 2nd edn., 2000.
[18] W. Schmickler, Interfacial Electrochemistry, Oxford University Press, 1st edn., 1996.
[19] H. N. Nong, L. J. Falling, A. Bergmann, M. Klingenhof, H. P. Tran, C. Spöri, R. Mom, J. Timoshenko, G. Zichittella, A. Knop-Gericke, S. Piccinin, J. Pérez-Ramírez, B. R. Cuenya, R. Schlögl, P. Strasser, D. Teschner and T. E. Jones, Nature, 2020, **587**, 408–413.
[20] K. H. Bevan, B. Miao and A. Iqbal, Comput. Phys. Comm., 2023, **286**, 108638.
[21] B. Klahr, S. Gimenez, F. Fabregat-Santiago, T. Hamann and J. Bisquert, J. Am. Chem. Soc, 2012, **134**, 4294–4302.
[22] B. Miao, K. Sangare, A. Iqbal, B. Marsan and K. H. Bevan, Phys. Chem. Chem. Phys., 2020, **22**, 19631–19642.
[23] A. Iqbal, M. S. Hossain and K. H. Bevan, Phys. Chem. Chem. Phys., 2016, **18**, 29466–29477.
[24] R. F. Pierret, Advanced Semiconductor Fundamentals, Pearson, 2nd edn., 2002.
[25] M. J. Cass, N. W. Duffy, K. Kirah, L. M. Peter, S. R. Pennock, S. Ushiroda and A. B. Walker, J. Electroanal. Chem., 2002, **538–539**, 191–203.
[26] W. W. Gartner, Phys. Rev., 1959, **116**, 84–86.
[27] K. H. Bevan, B. Miao and A. Iqbal, in Conversion of Water and CO_2 to Fuels using Solar Energy: Science, Technology and Materials, ed. O. K. Varghese and F. Leandro de Souza, Wiley, 2024.
[28] R. Pierret, Semiconductor Device Fundamentals, Pearson Education, 1996.
[29] Z. Zhao, Z. Li and Z. Zou, Phys. Chem. Chem. Phys., 2011, **13**, 4746.
[30] F. F. Abdi, T. J. Savenije, M. M. May, B. Dam and R. van de Krol, J. Phys. Chem. Lett., 2013, **4**, 2752.
[31] R. Crespo-Otero and A. Walsh, J. Phys. Chem. Lett., 2015, **6**, 2379.
[32] A. Iqbal and K. Bevan, MRS Commun., 2018, **8**, 466–473.
[33] K. Li, B. Miao, W. Fa, R. Chen, J. Jin, K. H. Bevan and D. Wang, ACS Appl. Mater. Interfaces, 2021, **13**, 17420–17428.
[34] Y. Gao and T. W. Hamann, J. Phys. Chem. Lett., 2017, **8**, 2700–2704.
[35] S. Datta, Quantum Transport: Atom to Transistor, Cambridge University Press, Cambridge, 2005.
[36] S. Luryi, Appl. Phys. Lett., 1988, **52**, 501.
[37] O. Zandi and T. W. Hamann, Nat. Chem., 2016, **8**, 778–783.
[38] C. Y. Cummings, F. Marken, L. M. Peter, K. G. Upul Wijayantha and A. A. Tahir, J. Am. Chem. Soc., 2012, **134**, 1228–1234.
[39] M. J. Cass, N. W. Duffy, L. M. Peter, S. R. Pennock, S. Ushiroda and A. B. Walker, The Journal of Physical Chemistry B, 2003, **107**, 5857–5863.
[40] A. V. Akimov and O. V. Prezhdo, Chem. Rev., 2015, **115**, 5797–5890.
[41] M. Patriarca, P. Farrell, J. Fuhrmann and T. Koprucki, Computer Physics Communications, 2019, **235**, 40–49.
[42] R. Sundararaman, D. Vigil-Fowler and K. Schwarz, Chem. Rev., 2022, **122**, 10651–10674.
[43] A. Iqbal and K. Bevan, J. Phys. Chem. C, 2018, **122**, 30–43.
[44] J. Fish, G. J. Wagner and S. Keten, Nature Materials, 2021, **20**, 774–786.